applied sciences

MDPI

Article

On Effective Bending Stiffness of a Laminate Nanoplate Considering Steigmann–Ogden Surface Elasticity

Victor A. Eremeyev [1,2,3,*] and Tomasz Wiczenbach [1]

[1] Faculty of Civil and Environmental Engineering, Gdańsk University of Technology, ul. Gabriela Narutowicza 11/12, 80-233 Gdańsk, Poland; tomasz.wiczenbach@pg.edu.pl
[2] Department of Civil and Environmental Engineering and Architecture (DICAAR), University of Cagliari, via Marengo, 2, 09123 Cagliari, Italy
[3] Research Institute for Mechanics, National Research Lobachevsky State University of Nizhny Novgorod, 23 Prospekt Gagarina (Gagarin Avenue) BLDG 6, 603950 Nizhny Novgorod, Russia
* Correspondence: vicereme@pg.edu.pl; Tel.: +48-58-347-1422

Received: 31 August 2020; Accepted: 18 October 2020; Published: 22 October 2020

Abstract: As at the nanoscale the surface-to-volume ratio may be comparable with any characteristic length, while the material properties may essentially depend on surface/interface energy properties. In order to get effective material properties at the nanoscale, one can use various generalized models of continuum. In particular, within the framework of continuum mechanics, the surface elasticity is applied to the modelling of surface-related phenomena. In this paper, we derive an expression for the effective bending stiffness of a laminate plate, considering the Steigmann–Ogden surface elasticity. To this end, we consider plane bending deformations and utilize the through-the-thickness integration procedure. As a result, the calculated elastic bending stiffness depends on lamina thickness and on bulk and surface elastic moduli. The obtained expression could be useful for the description of the bending of multilayered thin films.

Keywords: bending stiffness; laminate plate; surface elasticity; Steigmann–Ogden model; effective properties

1. Introduction

Nowadays, it is well established that the usual material properties at the nanoscale, such as Young's modulus, may significantly differ from what is observed at the macroscale. For example, Young's modulus becomes size-dependent; see, e.g., [1–3]. In other words, Young's modulus at the nanoscale depends on a specimen characteristic size. In fact, it describes the tensional stiffness of the considered specimen, which obviously can be size-dependent. In addition to tensional stiffness, there exist various other stiffness parameters such as bending and torsional stiffnesses, known from textbooks on the strength of materials. In particular, these parameters may characterize the behaviour of thin structures of nanometer size. For example, a bending stiffness can be directly measured using atomic force microscopy [4–6].

The idea of the bending stiffness of a plate belongs to Kirchhoff, who defined it as follows [7,8]

$$D = \frac{Eh^3}{12(1-\nu^2)}, \quad M = D\kappa, \tag{1}$$

where E and ν are Young's modulus and Poisson's ratio, h is the plate thickness, M is a bending moment, and κ is the curvature of a bent plate. By considering the bending of plates only, we can

restrict ourselves to two material parameters that are D and ν. So, in the "world of plates", D plays the role of an independent material parameter. In the literature, one can find various extensions of Kirchhoff's formula for more complex cases such as layered plates and plates with surface and interfacial stresses, etc.

The aim of this paper is to discuss the bending stiffness of layered nanosized plates. To this end, we consider the classic linear elasticity as a model for material properties in the bulk and the Steigmann–Ogden surface elasticity [9,10] for the modelling of plate faces and interfaces between layers. Let us note that surface elasticity models [9–12] were used for the modelling of surface-related phenomena and of nanometer-sized solids; see, e.g., [3,13–19] and references therein. When considering thin-walled structures, it is worth mentioning nonlocal models, which can also describe size effects. For the derivation of the governing equations of plates and shells using Eringen's type nonlocality, we refer to [20,21] and the references therein. Let us note tat the surface elasticity models can be treated as a singular case of nonlocality related to the appearance of boundary layers near shell faces. Similarities between the linear Gurtin–Murdoch model and the Toupin–Mindlin strain gradient elasticity were discussed in [16], whereas, in [22], a comparison with lattice dynamics was provided.

The paper is organized as follows. First, in Section 2, we briefly recall the basic governing equations of the Steigmann–Ogden surface elasticity. Here, we present the equilibrium equations in the bulk as well as the static boundary conditions derived through the Lagrange variational principle. In Section 3, we apply these equations to a laminate plate. By integrating trough-the-thickness, we obtain a layer-wise two-dimensional (2D) model of the plate. In order to find the bending stiffness of the whole plate, we consider a mean bending deflection in Section 4.

2. On the Steigmann–Ogden Surface Elasticity

Let us briefly introduce the Steigmann–Ogden surface elasticity in the case of infinitesimal deformations. We introduce the displacement vector as a differentiable vector function of the position vector $\mathbf{x}$

$$\mathbf{u} = \mathbf{u}(\mathbf{x}).$$

The constitutive relations of a hyperelastic solid can be expressed through the bulk $\mathcal{W}$ and surface $\mathcal{U}$ strain energies as follows

$$\mathcal{W} = \mathcal{W}(\mathbf{e}), \quad \mathcal{U} = \mathcal{U}(\boldsymbol{\varepsilon}, \boldsymbol{\kappa}). \tag{2}$$

Here, the strain measures in the bulk are given by

$$\mathbf{e} = \mathbf{e}(\mathbf{u}) = \tfrac{1}{2}(\nabla \mathbf{u} + \nabla \mathbf{u}^T),$$

whereas their surface counterparts take the form

$$\boldsymbol{\varepsilon} = \boldsymbol{\varepsilon}(\mathbf{u}) = \tfrac{1}{2}(\nabla_s \mathbf{u} \cdot \mathbf{P} + \mathbf{P} \cdot \nabla_s \mathbf{u}^T), \quad \boldsymbol{\kappa} = \boldsymbol{\kappa}(\mathbf{u}) = \tfrac{1}{2}(\nabla_s \boldsymbol{\vartheta} \cdot \mathbf{P} + \mathbf{P} \cdot \nabla_s \boldsymbol{\vartheta}^T), \quad \boldsymbol{\vartheta} = \boldsymbol{\vartheta}(\mathbf{u}) = \nabla_s w + \mathbf{B} \cdot \mathbf{u}.$$

Here, we introduce the spatial ∇ and surface ∇_s nabla operators, $\nabla_s = \mathbf{P} \cdot \nabla$, $\mathbf{P} = \mathbf{I} - \mathbf{n} \otimes \mathbf{n}$, where $\mathbf{I}$ is the 3D unit tensor, "$(...)^T$" denotes the transpose of a second-order tensor $(...)$, and "$\cdot$" and "$\otimes$" stand for the scalar and dyadic products, respectively. In addition, $w = \mathbf{u} \cdot \mathbf{n}$, $\mathbf{B} = -\nabla_s \mathbf{n}$ is the tensor of curvature and $\mathbf{n}$ is the normal outward unit to the body boundary $S \equiv \partial V$. Hereinafter, we use the direct (coordinate-free) tensor calculus as in [23,24].

In what follows we consider isotropic solids, so $\mathcal{W}$ and the stress tensor $\boldsymbol{\sigma}$ are defined by

$$\mathcal{W} = \tfrac{1}{2}\mathbf{e} : \mathbf{C} : \mathbf{e}, \quad \boldsymbol{\sigma} = \frac{\partial \mathcal{W}}{\partial \mathbf{e}} = \mathbf{C} : \mathbf{e},$$

where $\mathbf{C}$ is a forth-order elastic moduli tensor given by

$$\mathbf{C} = C_{ijkl}\mathbf{i}_i \otimes \mathbf{i}_j \otimes \mathbf{i}_k \otimes \mathbf{i}_l, \quad C_{ijkl} = \lambda\delta_{ij}\delta_{kl} + \mu\left(\delta_{ik}\delta_{jl} + \delta_{il}\delta_{jk}\right), \tag{3}$$

where δ_{ij} is the Kronecker symbol, $\mathbf{i}_k$ are unit Cartesian base vectors, λ and μ are the Lamé elastic moduli, and ":" stands for the inner product in the space of second-order tensors.

The surface strain energy can be written in the form [9,10,25]

$$\mathcal{U} = \mu^S\boldsymbol{\varepsilon} : \boldsymbol{\varepsilon} + \tfrac{1}{2}\lambda^S \mathrm{tr}^2\boldsymbol{\varepsilon} + \eta\boldsymbol{\kappa} : \boldsymbol{\kappa} + \tfrac{1}{2}\chi \mathrm{tr}^2\boldsymbol{\kappa}, \tag{4}$$

where λ^S and μ^S are the surface Lamé moduli, χ and η are additional stiffness moduli related to the bending stiffness of the material surface with surface stresses, and tr is the trace operator.

By considering the determination of the surface elastic moduli in (4), we can use such estimations as

$$\mu^S \approx \bar{\mu}h_S, \quad \eta \approx \bar{\mu}h_S^3, \quad \text{etc.},$$

where $\bar{\mu}$ is a shear modulus of a material in the vicinity of a free interface or an interface and h_S is the thickness of the surface/interfacial layer. In other words, we have here the so-called static characteristic length scale parameter, defined as μ^S/μ. For more detail, we refer readers to [17,19], where recent discussions on the evaluation of surface elastic moduli are provided and relative references are presented. In particular, in [17,19] it was mentioned that the linear Gurtin–Murdoch model corresponds to so-called stiff interfaces discussed earlier in [26,27] or plates with rigid skins [28].

In order to obtain the equilibrium equations and the natural boundary conditions, we use the Lagrange variational principle, modified for the presence of the surface energy [25,29]. Here, the functional is defined as follows

$$\mathbb{L}[\mathbf{u}] = \mathbb{B}[\mathbf{u}] + \mathbb{S}[\mathbf{u}], \quad \mathbb{B}[\mathbf{u}] = \int_V \mathcal{W}(\mathbf{e}(\mathbf{u}))\ \mathrm{d}V, \quad \mathbb{S}[\mathbf{u}] = \int_A \mathcal{U}(\boldsymbol{\varepsilon}(\mathbf{u}), \boldsymbol{\kappa}(\mathbf{u}))\ \mathrm{d}S. \tag{5}$$

In (5), $\mathbb{B}$ and $\mathbb{S}$ are the energy and surface energy functionals, respectively. Here $A \subset S \equiv \partial V$, is the part of the boundary or interface where the surface stresses are defined. The work of external loads has the standard form

$$\delta\mathbb{A}[\delta\mathbf{u}] = \int_V \rho\mathbf{f}\cdot\delta\mathbf{u}\ \mathrm{d}V + \int_A \mathbf{t}\cdot\delta\mathbf{u}\ \mathrm{d}S,$$

where ρ is the mass density, $\mathbf{f}$ and $\mathbf{t}$ are vectors of mass force and surface traction, respectively.

Using the standard technique of the calculus of variations from the variational equation

$$\delta\mathbb{L} = \delta\mathbb{A}$$

we derive the equilibrium equations and the natural boundary conditions at A

$$\nabla\cdot\boldsymbol{\sigma} + \rho\mathbf{f} = \mathbf{0}, \tag{6}$$

$$\mathbf{n}\cdot\boldsymbol{\sigma} = \nabla_s\cdot[\mathbf{T} - (\nabla_s\cdot\mathbf{M})\mathbf{n}] - 2H\mathbf{n}\cdot(\nabla_s\cdot\mathbf{M})\mathbf{n} + \mathbf{t}, \tag{7}$$

where $H = -\frac{1}{2}\nabla_s\cdot\mathbf{n}$ is the mean curvature of A, and we introduc the surface stress $\mathbf{T}$ and surface hyperstress $\mathbf{M}$ tensors by

$$\mathbf{T} = \frac{\partial\mathcal{U}}{\partial\boldsymbol{\varepsilon}}, \quad \mathbf{M} = \frac{\partial\mathcal{U}}{\partial\boldsymbol{\kappa}}.$$

Equations (6) and (7) include, as a particular case, equilibrium conditions for simple materials without surface stresses, and with surface stresses, defined as in the Gurtin–Murdoch model. An extension of these conditions for dynamics and for strain gradient continua is given in [29,30].

3. Laminate Plate

In what follows, using relations (6) and (7), we consider the equilibrium conditions of an N-layered plate; see Figure 1. For the plate, we introduce $2N+1$ constitutive relations for N layers, for two faces and for $N-1$ interfaces

$$\mathcal{W} = \mathcal{W}_i(\mathbf{e}(\mathbf{u}_i)), \quad \mathcal{U} = \mathcal{U}_0(\boldsymbol{\varepsilon}(\mathbf{u}_0), \boldsymbol{\kappa}(\mathbf{u}_0)), \quad \mathcal{U} = \mathcal{U}_i(\boldsymbol{\varepsilon}(\mathbf{u}_i), \boldsymbol{\kappa}(\mathbf{u}_i)), \qquad i = 1, \ldots, N,$$

where $\mathbf{u}_k$ and $k = 0, \ldots, N$, are corresponding vectors of displacements. Let the i-th layer be of thickness h_i, so the total thickness h of the plate is given by

$$h = \sum_{i=1}^{N} h_i.$$

In addition to the Cartesian coordinates x, y, $(x, y) \in \Omega$, $z \in [0, h]$, with the unit base vectors $\mathbf{i}_1$, $\mathbf{i}_2$, $\mathbf{i}_3$, for the i-th layer, we introduce a local coordinate ζ_i such that

$$\zeta_i = z - z_i,$$

where z_i is the coordinate of the middle plane of the i-th layer,

$$z_1 = \tfrac{1}{2}h_1, \quad z_j = \tfrac{1}{2}h_j + \sum_{k=1}^{j-1} h_k, \quad j > 1.$$

Thus, we get $\zeta_i \in [-h_i/2, h_i/2]$.

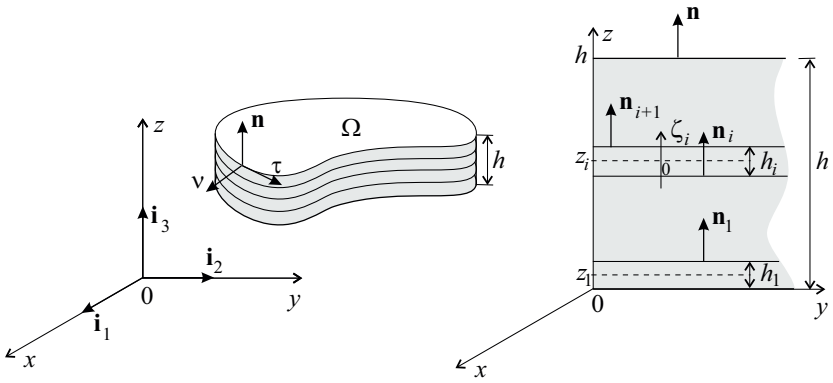

Figure 1. Nth layered plate of thickness h. Here $N = 4$, and the ith layer has a thickness of h_i, $i = 1, \ldots..., N$.

As a result, functionals $\mathbb{B}$ and $\mathbb{S}$ take the form

$$\mathbb{B}[\mathbf{u}] = \int_V \mathcal{W}(\mathbf{e}(\mathbf{u}))\, \mathrm{d}V = \int_0^h \int_\Omega \mathcal{W}\, \mathrm{d}S\, \mathrm{d}z = \sum_{i=1}^{N} \int_{z_i - h_i/2}^{z_i + h_i/2} \left(\int_\Omega \mathcal{W}_i\, \mathrm{d}S \right) \mathrm{d}z$$

$$= \sum_{i=1}^{N} \int_{-h_i/2}^{h_i/2} \left(\int_\Omega \mathcal{W}_i\, \mathrm{d}S \right) \mathrm{d}\zeta_i, \tag{8}$$

$$\mathbb{S}[\mathbf{u}] = \int_A \mathcal{U}(\boldsymbol{\varepsilon}(\mathbf{u}), \boldsymbol{\kappa}(\mathbf{u}))\, \mathrm{d}S = \sum_{i=0}^{N} \int_\Omega \mathcal{U}_i\, \mathrm{d}S. \tag{9}$$

Let us note that, for a plate geometry, we make significant simplifications to the formulae. In particular, here we get $H = 0,\ \mathrm{d}S = \mathrm{d}x\,\mathrm{d}y$ and

$$\nabla = \mathbf{i}_1\frac{\partial}{\partial x} + \mathbf{i}_2\frac{\partial}{\partial y} + \mathbf{i}_3\frac{\partial}{\partial z}, \quad \nabla_s = \mathbf{i}_1\frac{\partial}{\partial x} + \mathbf{i}_2\frac{\partial}{\partial y}.$$

In other words, for each surface with surface stresses, we can apply the same 2D nabla-operator. As a result, for a laminate plate, we get the equilibrium equations

$$\nabla \cdot \boldsymbol{\sigma}_i + \rho_i \mathbf{f} = \mathbf{0}, \tag{10}$$

boundary conditions on faces $z = 0$ and $z = h$ in the simplified form of (7)

$$\mathbf{n}\cdot\boldsymbol{\sigma}_0 = \nabla_s \cdot [\mathbf{T}_0 - (\nabla_s \cdot \mathbf{M}_0)\mathbf{n}] + \mathbf{t}_0, \quad \mathbf{n}\cdot\boldsymbol{\sigma}_N = \nabla_s \cdot [\mathbf{T}_N - (\nabla_s \cdot \mathbf{M}_N)\mathbf{n}] + \mathbf{t}_N,$$

and the compatibility conditions on the interfaces $z = h_i$, $i = 1, \dots N-1$

$$\mathbf{n}\cdot[\![\boldsymbol{\sigma}]\!] = \nabla_s \cdot [\mathbf{T}_i - (\nabla_s \cdot \mathbf{M}_i)\mathbf{n}]\,.$$

Here, $[\![(\dots)]\!]$ means the discontinuity jump across an interface.

These equations constitute an exact 3D boundary value problem for the laminate plate. For 3D-to-2D reduction, we can use various techniques resulting in a system of 2D governing equations; see, e.g., the recent review [31]. On the other hand, let us recall that the main aim of this paper is to determine the effective total bending stiffness of a laminate plate while considering surface elasticity. To this end, it is enough to consider a particular class of deformations related to pure bending. By considering $\mathbb{L} = \mathbb{B} + \mathbb{S}$ on these deformations, we can estimate the bending stiffness as a stiffness coefficient related to changes in the mean curvature of the plate.

4. Effective Bending Stiffness

Let us consider possible approximations of displacement fields $\mathbf{u}_i$, $i = 1, 2, \dots N$. In order to illustrate an idea, we begin from a one-layer plate with surface stresses.

4.1. One-Layered Plate with Surface Stresses

First, we recall the linear theory of plate bending without surface stresses [8]. The bending deformation of an homogeneous plate ($N = 1$) is given by

$$\mathbf{u}(x,y,z) = v_1(x,y,z)\mathbf{i}_1 + v_2(x,y,z)\mathbf{i}_2 + w(x,y)\mathbf{i}_3, \tag{11}$$

where

$$v_1 = -z\frac{\partial w}{\partial x}, \quad v_2 = -z\frac{\partial w}{\partial y}$$

are in-plane displacements and w is a deflection. Under plane stress conditions, the 2D strain energy density takes the form

$$\mathbb{E}_B \equiv \int_{-h/2}^{h/2} \mathcal{W}\,\mathrm{d}\zeta = \frac{1}{2}D\left[\left(\frac{\partial^2 w}{\partial x^2}\right)^2 + \left(\frac{\partial^2 w}{\partial y^2}\right)^2 + 2\nu\frac{\partial^2 w}{\partial x^2}\frac{\partial^2 w}{\partial y^2}\right], \tag{12}$$

where D is defined in (1).

By assuming cylindrical bending with $w = w(x) = \frac{1}{2}\kappa x^2$, we have the formulae

$$\mathbf{u} = -z\frac{\partial w}{\partial x}\mathbf{i}_1 + w\mathbf{i}_3 = -z\kappa x\mathbf{i}_1 + \frac{1}{2}\kappa x^2\mathbf{i}_3, \tag{13}$$

$$\nabla\mathbf{u} = -\frac{\partial w}{\partial x}\mathbf{i}_3\otimes\mathbf{i}_1 - z\frac{\partial^2 w}{\partial x^2}\mathbf{i}_1\otimes\mathbf{i}_1 + \frac{\partial w}{\partial x}\mathbf{i}_1\otimes\mathbf{i}_3 = -\kappa x\mathbf{i}_3\otimes\mathbf{i}_1 - z\kappa\mathbf{i}_1\otimes\mathbf{i}_1 + \kappa x\mathbf{i}_1\otimes\mathbf{i}_3, \tag{14}$$

$$\mathbf{e} = \boldsymbol{\varepsilon} = -z\frac{\partial^2 w}{\partial x^2}\mathbf{i}_1\otimes\mathbf{i}_1 = -\kappa z\mathbf{i}_1\otimes\mathbf{i}_1, \tag{15}$$

$$\boldsymbol{\vartheta} = \frac{\partial w}{\partial x}\mathbf{i}_1 = \kappa x\mathbf{i}_1, \quad \boldsymbol{\kappa} = \frac{\partial^2 w}{\partial x^2}\mathbf{i}_1\otimes\mathbf{i}_1 = \kappa\mathbf{i}_1\otimes\mathbf{i}_1. \tag{16}$$

With these formulae, we get the simplified formula for $\mathbb{E}_B$

$$\mathbb{E}_B = \frac{1}{2}D\kappa^2.$$

Thus, D can be calculated as follows

$$D = \frac{\partial^2\mathbb{E}_B}{\partial\kappa^2}. \tag{17}$$

Now let us consider surface energy functional $\mathbb{S}$ given by (9) for $N = 1$. We get

$$\begin{aligned}\mathbb{E}_S =& \mathcal{U}_0\Big|_{z=-h/2} + \mathcal{U}_1\Big|_{z=h/2}\\ =& \frac{1}{2}\left[(2\mu_0^S + \lambda_0^S)\frac{h^2}{4} + 2\eta_0 + \chi_0\right]\kappa^2 + \frac{1}{2}\left[(2\mu_1^S + \lambda_1^S)\frac{h^2}{4} + 2\eta_1 + \chi_1\right]\kappa^2.\end{aligned} \tag{18}$$

As a result, the total 2D surface strain density takes the following form

$$\mathbb{E} \equiv \mathbb{E}_B + \mathbb{E}_S = \frac{1}{2}D_{\text{eff}}\kappa^2, \tag{19}$$

where the effective bending stiffness is given by

$$D_{\text{eff}} = D + (2\mu_0^S + \lambda_0^S)\frac{h^2}{4} + 2\eta_0 + \chi_0 + (2\mu_1^S + \lambda_1^S)\frac{h^2}{4} + 2\eta_1 + \chi_1. \tag{20}$$

Obviously, the surface bending stiffness parameters η_i and χ_i make a contribution to the effective bending stiffness, as it should be. Equation (20) contains also the expression of the effective bending stiffness obtained within the Gurtin–Murdoch surface elasticity [32]. Dimensionless bending stiffness as function of the plate thickness h is given in Figure 2. Here, $\overline{D} = D_{\text{eff}}/D$ and we define the characteristic length l as in the case of the Gurtin–Murdoch model $l = (\lambda^S + 2\mu)h^2/D$. Obviously, the surface bending stiffness, taken into account within the Steigmann–Ogden model, leads to an increase in the effective bending stiffness in comparison with the Gurtin–Murdoch model or the classic Kirchhoff bending stiffness. This influence is essential when $h \lesssim 5l$.

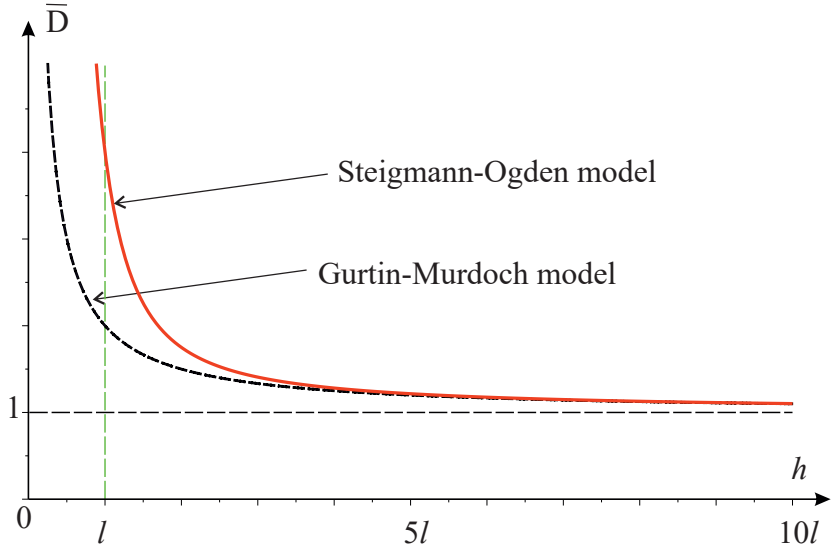

Figure 2. Dimensionless bending stiffness $\overline{D} = D_{\text{eff}}/D$ vs. thickness h (solid red curve). The dashed blue curve corresponds to the Gurtin–Murdoch model; the horizonal dashed black line describes the classic bending stiffness. Finally, the vertical dashed green line marks the characteristic length l defined as $l = (\lambda^S + 2\mu)h^2/D$.

4.2. Three-Layered Plate with Surface Stresses

Let us consider the three-layered plate, which is symmetric in the thickness direction, $N = 3$. In this case, the core thickness is $h_c = h_2$, whereas the faces have the same thickness $h_1 = h_3 = h_f/2$, so we have $h = h_c + h_f$. The effective bending stiffness of the three-layered plate without surface stresses, calculated within the first-order shear deformable plate model, is given by [33]

$$D^0_{eff} = \frac{1}{2}\left\langle \frac{Ez^2}{1-\nu} \right\rangle + \frac{1}{2}\left\langle \frac{Ez^2}{1+\nu} \right\rangle, \qquad \langle(\ldots)\rangle = \int_{-h/2}^{h/2} (\ldots)\,\mathrm{d}z, \tag{21}$$

which results in

$$D^0_{eff} = \frac{1}{12}\left[\frac{E_f(h^3 - h_c^3)}{1-\nu_f^2} + \frac{E_c h_c^3}{1-\nu_c^2}\right], \tag{22}$$

where E_f and ν_f, E_c and ν_c are Young's modulus and Poisson's ratio of faces and core, respectively. Thus, we have

$$\mathbb{E}_B = \frac{1}{2} D^0_{eff} \kappa^2.$$

By considering surface stresses, we get

$$\begin{aligned}
\mathbb{E}_S =& \mathcal{U}_0\Big|_{z=-h/2} + \mathcal{U}_1\Big|_{z=-h_c/2} + \mathcal{U}_2\Big|_{z=h_c/2} + \mathcal{U}_3\Big|_{z=h/2} \\
=& \frac{1}{2}\left[(2\mu_0^S + \lambda_0^S)\frac{h^2}{4} + 2\eta_0 + \chi_0\right]\kappa^2 \\
&+ \frac{1}{2}\left[(2\mu_1^S + \lambda_1^S)\frac{h_c^2}{4} + 2\eta_1 + \chi_1\right]\kappa^2 \\
&+ \frac{1}{2}\left[(2\mu_2^S + \lambda_2^S)\frac{h_c^2}{4} + 2\eta_2 + \chi_2\right]\kappa^2 \\
&+ \frac{1}{2}\left[(2\mu_3^S + \lambda_3^S)\frac{h^2}{4} + 2\eta_3 + \chi_3\right]\kappa^2.
\end{aligned} \tag{23}$$

As a result, the effective bending stiffness becomes

$$\begin{aligned} D_{eff} =& D^0_{eff} + D^{GM}_{eff} + D^{SO}_{eff}, \\ D^{GM}_{eff} =& (2\mu_0^S + \lambda_0^S)\frac{h^2}{4} + (2\mu_1^S + \lambda_1^S)\frac{h_c^2}{4} + (2\mu_2^S + \lambda_2^S)\frac{h_c^2}{4} + (2\mu_3^S + \lambda_3^S)\frac{h^2}{4}, \\ D^{SO}_{eff} =& \sum_{i=0}^{3} (2\eta_i + \chi_i)\,. \end{aligned} \tag{24}$$

where D^{GM}_{eff} is the contribution to the effective bending stiffness in the framework of the Gurtin–Murdoch model and D^{SO}_{eff} is the additional term related to the surface bending stiffness in the framework of the Steigmann–Ogden model.

4.3. N-Layered Plate with Surface Stresses

A similar approach can be applied to multi-layered plate. In order to get the effective bending stiffness, we calculate the 2D strain energy density $\mathbb{E}$. Here, D^0_{eff} is given by (21), whereas $\mathbb{S}_S$ can be calculated as follows

$$\mathbb{E}_S = \mathcal{U}_0\Big|_{z=-h/2} + \sum_{i=1}^{N} \mathcal{U}_i\Big|_{z=-h/2+\sum_{k=1}^{i} h_k}, \tag{25}$$

which results in the following formulae

$$D^{GM}_{eff} = (2\mu_0^S + \lambda_0^S)\frac{h^2}{4} + \sum_{i=1}^{N}(2\mu_i^S + \lambda_i^S)\frac{z^2}{4}\Big|_{z=-h/2+\sum_{k=1}^{i} h_k}, \quad D^{SO}_{eff} = \sum_{i=0}^{N} (2\eta_i + \chi_i)\,. \tag{26}$$

As an example, let us consider a multilayered plate with layers of equal thickness and equal properties, i.e., $h_i = t \equiv h/N$, $\mu_i^S = \mu^S$, $\lambda_i^S = \lambda^S$, $\eta_i = \eta$, $\chi_i = \chi$, $i = 0, 1, \ldots, N$. In this case, $D^0_{eff} = D$, whereas

$$D^{GM}_{eff} = (2\mu^S + \lambda^S)\frac{t^2}{4}\sum_{i=0}^{N}(i - N/2)^2, \quad D^{SO}_{eff} = (N+1)\,(2\eta + \chi)\,,$$

and

$$D_{eff} = \frac{Eh^3}{12(1-\nu^2)} + \frac{1}{N}\left(\frac{1}{6}N^2 + \frac{1}{2}N + \frac{1}{3}\right)(2\mu^S + \lambda^S)\frac{h^2}{8} + (N+1)\,(2\eta + \chi)\,. \tag{27}$$

where we use the formula

$$\sum_{i=0}^{N}(i - N/2)^2 = \frac{1}{12}N^3 + \frac{1}{4}N^2 + \frac{1}{6}N.$$

For $N = 1$ and $N = 3$, i.e., for homogeneous and three-layered plates, Equation (27) reduces to (20) and to (24), respectively. The characteristic dependencies of the dimensionless stiffness $\overline{D}$ on N are given in Figure 3 for $N = 1, 5, 10, 20$. The horizontal dashed lines have the same meaning as in Figure 2.

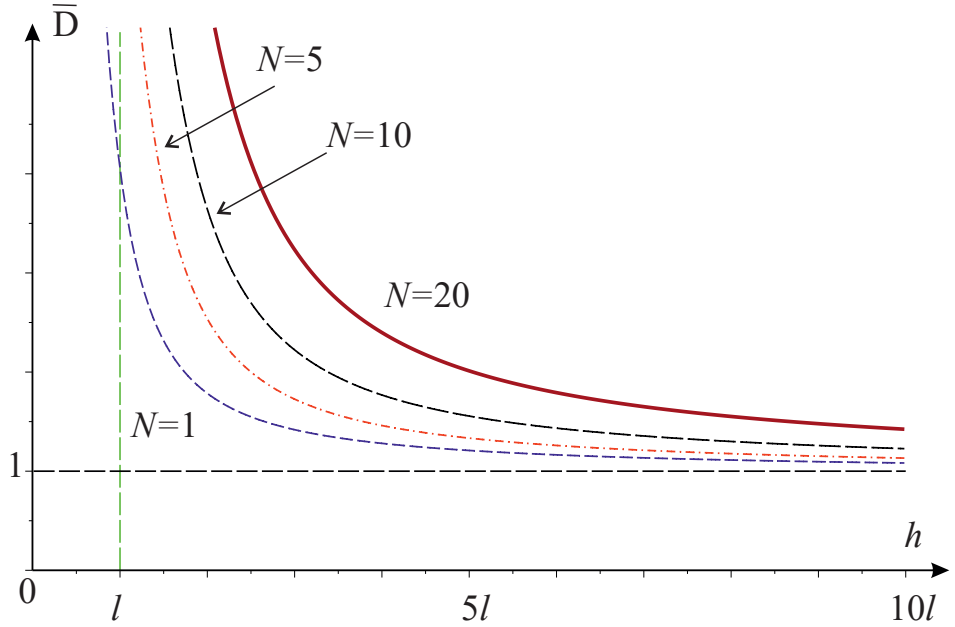

Figure 3. Dimensionless bending stiffness $\overline{D}$ vs. number of layers N.

5. Discussion and Conclusions

Here, we have derived the effective bending stiffness of multilayered plate by considering surface stresses as in the Steigmann–Ogden model of surface elasticity. Unlike the Gurtin–Murdoch model, this model explicitly takes into account the surface bending stiffness. As a result, the derived formula contains various contributions related to the elastic response in the bulk, the influence of the surface Lamé moduli and of the surface bending stiffness moduli. For the Nth-layered plate, the effective bending stiffness depends on N (see (26) or (27)), so the influence of the surface moduli is more pronounced, especially for plates of nano-sized thickness. Here, we restricted ourselves to the determination of the effective bending stiffness and the analysis of the surface bending stiffness influence. The complete theory of multilayered plates can be developed using layer-wise theory as in [34,35], where D_{eff} can be considered as a global stiffness characteristic of the whole laminate plate.

The bending of a multilayered plate presents a natural example of the influence of the surface bending stiffness, which is a peculiarity of the Steigmann–Ogden model. Among other examples of this kind, let us mention the bending of dominant beam–lattice structures such as those considered in [18] for the Gurtin–Murdoch model, or porous materials such as those analyzed in [2,3,36,37]. Due to their very good prospective properties, such beam–lattice structures have found various applications in engineering; see, e.g., [38–41] for pantographic beam–lattice materials including pantographic beams [42–45] and plates [46–48]. Indeed, by considering surface elasticity, we can see that this may change the response at the micro- and nanoscale; thus, for beam–lattices at small scales, as presented in [49], the surface bending stiffness may play a dominant role.

Author Contributions: Conceptualization, V.A.E.; methodology, V.A.E.; software, V.A.E.; validation, V.A.E. and T.W.; formal analysis, V.A.E.; investigation, V.A.E. and T.W.; writing—original draft preparation, V.A.E. and T.W.; writing—review and editing, V.A.E.; visualization, T.W.; supervision, V.A.E.; project administration, V.A.E.; funding acquisition, V.A.E. All authors have read and agreed to the published version of the manuscript.

Funding: This research was funded by a grant from the Government of the Russian Federation (contract No. 14.Y26.31.0031). The APC was funded by the International Research Center for Mathematics & Mechanics of Complex Systems (M&MoCS) of the University dell'Aquila, Italy.

Conflicts of Interest: The authors declare no conflict of interest.

References

1. Miller, R.E.; Shenoy, V.B. Size-dependent elastic properties of nanosized structural elements. *Nanotechnology* **2000**, *11*, 139–147. [CrossRef]
2. Wang, J.; Duan, H.L.; Huang, Z.P.; Karihaloo, B.L. A scaling law for properties of nano-structured materials. *Proc. R. Soc. Lond. A* **2006**, *462*, 1355–1363. [CrossRef]
3. Duan, H.L.; Wang, J.; Karihaloo, B.L. Theory of Elasticity at the Nanoscale. In *Advances in Applied Mechanic*; Elsevier: Amsterdam, The Netherlands, 2008; Volume 42, pp. 1–68.
4. Kis, A.; Kasas, S.; Babic, B.; Kulik, A.J.; Benoit, W.; Briggs, G.; Schonenberger, C.; Catsicas, S.; Forro, L. Nanomechanics of microtubules. *Phys. Rev. Lett.* **2002**, *89*, 248101.
5. Jing, G.Y.; Duan, H.L.; Sun, X.M.; Zhang, Z.S.; Xu, J.; Li, Y.D.; Wang, J.X.; Yu, D.P. Surface effects on elastic properties of silver nanowires: Contact atomic-force microscopy. *Phys. Rev. B* **2006**, *73*, 235409–235416. [CrossRef]
6. Pustan, M.; Birleanu, C.; Dudescu, C. Nanocharacterization of the adhesion effect and bending stiffness in optical MEMS. *Appl. Surf. Sci.* **2017**, *421*, 191–199. [CrossRef]
7. Kirchhoff, G.R. Über das Gleichgewicht und die Bewegung einer elastischen Scheibe. *Crelles J. Für Die Reine Und Angew. Math.* **1850**, *40*, 51–88.
8. Timoshenko, S.P.; Woinowsky-Krieger, S. *Theory of Plates and Shells*; McGraw Hill: New York, NY, USA, 1985.
9. Steigmann, D.J.; Ogden, R.W. Plane deformations of elastic solids with intrinsic boundary elasticity. *Proc. R. Soc. A* **1997**, *453*, 853–877. [CrossRef]
10. Steigmann, D.J.; Ogden, R.W. Elastic surface-substrate interactions. *Proc. R. Soc. A* **1999**, *455*, 437–474. [CrossRef]
11. Gurtin, M.E.; Murdoch, A.I. A continuum theory of elastic material surfaces. *Arch. Ration. Mech. Anal.* **1975**, *57*, 291–323. [CrossRef]
12. Gurtin, M.E.; Murdoch, A.I. Surface stress in solids. *Int. J. Solids Struct.* **1978**, *14*, 431–440. [CrossRef]
13. Wang, J.; Huang, Z.; Duan, H.; Yu, S.; Feng, X.; Wang, G.; Zhang, W.; Wang, T. Surface stress effect in mechanics of nanostructured materials. *Acta Mech. Solida Sin.* **2011**, *24*, 52–82. [CrossRef]
14. Zemlyanova, A.Y.; Mogilevskaya, S.G. Circular inhomogeneity with Steigmann–Ogden interface: Local fields, neutrality, and Maxwell's type approximation formula. *Int. J. Solids Struct.* **2018**, *135*, 85–98. [CrossRef]
15. Han, Z.; Mogilevskaya, S.G.; Schillinger, D. Local fields and overall transverse properties of unidirectional composite materials with multiple nanofibers and Steigmann–Ogden interfaces. *Int. J. Solids Struct.* **2018**, *147*, 166–182. [CrossRef]
16. Eremeyev, V.A.; Rosi, G.; Naili, S. Comparison of anti-plane surface waves in strain-gradient materials and materials with surface stresses. *Math. Mech. Solids* **2019**, *24*, 2526–2535. [CrossRef]
17. Eremeyev, V.A.; Rosi, G.; Naili, S. Transverse surface waves on a cylindrical surface with coating. *Int. J. Eng. Sci.* **2020**, *147*, 103188. [CrossRef]
18. Rahali, Y.; Eremeyev, V.A.; Ganghoffer, J.F. Surface effects of network materials based on strain gradient homogenized media. *Math. Mech. Solids* **2020**, *25*, 389–406. [CrossRef]
19. Gorbushin, N.; Eremeyev, V.A.; Mishuris, G. On stress singularity near the tip of a crack with surface stresses. *Int. J. Eng. Sci.* **2020**, *146*, 103183. [CrossRef]
20. Chebakov, R.; Kaplunov, J.; Rogerson, G.A. A non-local asymptotic theory for thin elastic plates. *Proc. R. Soc. A Math. Phys. Eng. Sci.* **2017**, *473*, 20170249. [CrossRef]
21. Sajadi, B.; Goosen, H.; van Keulen, F. Capturing the effect of thickness on size-dependent behavior of plates with nonlocal theory. *Int. J. Solids Struct.* **2017**, *115-116*, 140 – 148. [CrossRef]
22. Eremeyev, V.A.; Sharma, B.L. Anti-plane surface waves in media with surface structure: Discrete vs. continuum model. *Int. J. Eng. Sci.* **2019**, *143*, 33–38. [CrossRef]
23. Simmonds, J.G. *A Brief on Tensor Analysis*, 2nd ed.; Springer: New York, NY, USA, 1994.
24. Eremeyev, V.A.; Cloud, M.J.; Lebedev, L.P. *Applications of Tensor Analysis in Continuum Mechanics*; World Scientific: Singapore, 2018.
25. Eremeyev, V.A.; Lebedev, L.P. Mathematical study of boundary-value problems within the framework of Steigmann–Ogden model of surface elasticity. *Contin. Mech. Thermodyn.* **2016**, *28*, 407–422. [CrossRef]
26. Benveniste, Y.; Miloh, T. Imperfect soft and stiff interfaces in two-dimensional elasticity. *Mech. Mater.* **2001**, *33*, 309–323. [CrossRef]

27. Mishuris, G.S.; Movchan, N.V.; Movchan, A.B. Steady-state motion of a mode-III crack on imperfect interfaces. *Q. J. Mech. Appl. Math.* **2006**, *59*, 487–516. [CrossRef]
28. Berdichevsky, V.L. Nonlinear theory of hard-skin plates and shells. *Int. J. Eng. Sci.* **2010**, *48*, 357–369. [CrossRef]
29. Eremeyev, V.A. On dynamic boundary conditions within the linear Steigmann-Ogden model of surface elasticity and strain gradient elasticity. In *Dynamical Processes in Generalized Continua and Structures*; Altenbach, H., Belyaev, A., Eremeyev, V.A., Krivtsov, A., Porubov, A.V., Eds.; Springer: Cham, Switzerland, 2019; pp. 195–207.
30. Abali, B.E.; Müller, W.H.; dell'Isola, F. Theory and computation of higher gradient elasticity theories based on action principles. *Arch. Appl. Mech.* **2017**, *87*, 1495–1510. [CrossRef]
31. Altenbach, H.; Eremeyev, V. Thin-Walled Structural Elements: Classification, Classical and Advanced Theories, New Applications. In *Shell-like Structures: Advanced Theories and Applications*; Altenbach, H., Eremeyev, V., Eds.; Springer International Publishing: Cham, Switzerland, 2017; pp. 1–62.
32. Altenbach, H.; Eremeyev, V.A. On the shell theory on the nanoscale with surface stresses. *Int. J. Eng. Sci.* **2011**, *49*, 1294–1301. [CrossRef]
33. Altenbach, H.; Eremeyev, V.A. Direct approach-based analysis of plates composed of functionally graded materials. *Arch. Appl. Mech.* **2008**, *78*, 775–794. [CrossRef]
34. Naumenko, K.; Eremeyev, V.A. A layer-wise theory for laminated glass and photovoltaic panels. *Compos. Struct.* **2014**, *112*, 283–291. [CrossRef]
35. Naumenko, K.; Eremeyev, V.A. A layer-wise theory of shallow shells with thin soft core for laminated glass and photovoltaic applications. *Compos. Struct.* **2017**, *178*, 434–446. [CrossRef]
36. dell'Isola, F.; Guarascio, M.; Hutter, K. A variational approach for the deformation of a saturated porous solid. A second-gradient theory extending Terzaghi's effective stress principle. *Arch. Appl. Mech.* **2000**, *70*, 323–337. [CrossRef]
37. Casalotti, A.; D'Annibale, F.; Rosi, G. Multi-scale design of an architected composite structure with optimized graded properties. *Compos. Struct.* **2020**, *252*, 112608. [CrossRef]
38. dell'Isola, F.; Giorgio, I.; Pawlikowski, M.; Rizzi, N.L. Large deformations of planar extensible beams and pantographic lattices: Heuristic homogenization, experimental and numerical examples of equilibrium. *Proc. R. Soc. A Math. Phys. Eng. Sci.* **2016**, *472*, 20150790. [CrossRef]
39. Turco, E.; Golaszewski, M.; Giorgio, I.; D'Annibale, F. Pantographic lattices with non-orthogonal fibres: Experiments and their numerical simulations. *Compos. Part B Eng.* **2017**, *118*, 1–14. [CrossRef]
40. Dell'Isola, F.; Seppecher, P.; Alibert, J.J.; Lekszycki, T.; Grygoruk, R.; Pawlikowski, M.; Steigmann, D.; Giorgio, I.; Andreaus, U.; Turco, E.; et al. Pantographic metamaterials: An example of mathematically driven design and of its technological challenges. *Contin. Mech. Thermodyn.* **2019**, *31*, 851–884. [CrossRef]
41. Dell'Isola, F.; Seppecher, P.; Spagnuolo, M.; Barchiesi, E.; Hild, F.; Lekszycki, T.; Giorgio, I.; Placidi, L.; Andreaus, U.; Cuomo, M.; et al. Advances in pantographic structures: Design, manufacturing, models, experiments and image analyses. *Contin. Mech. Thermodyn.* **2019**, *31*, 1231–1282. [CrossRef]
42. Alibert, J.J.; Seppecher, P.; dell'Isola, F. Truss modular beams with deformation energy depending on higher displacement gradients. *Math. Mech. Solids* **2003**, *8*, 51–73. [CrossRef]
43. Turco, E.; Barchiesi, E. Equilibrium paths of Hencky pantographic beams in three-point bending problem. *Math. Mech. Complex Syst.* **2019**, *7*, 287–310. [CrossRef]
44. Barchiesi, E.; Eugster, S.R.; Placidi, L.; dell'Isola, F. Pantographic beam: A complete second gradient 1D-continuum in plane. *Z. Für Angew. Math. Und Phys.* **2019**, *70*, 135. [CrossRef]
45. Eremeyev, V.A.; Ganghoffer, J.F.; Konopińska-Zmysłowska, V.; Uglov, N.S. Flexoelectricity and apparent piezoelectricity of a pantographic micro-bar. *Int. J. Eng. Sci.* **2020**, *149*, 103213. [CrossRef]
46. Scerrato, D.; Giorgio, I.; Rizzi, N.L. Three-dimensional instabilities of pantographic sheets with parabolic lattices: Numerical investigations. *Z. Für Angew. Math. Und Phys.* **2016**, *67*, 53. [CrossRef]
47. Giorgio, I.; Rizzi, N.; Turco, E. Continuum modelling of pantographic sheets for out-of-plane bifurcation and vibrational analysis. *Proc. R. Soc. A Math. Phys. Eng. Sci.* **2017**, *473*, 20170636. [CrossRef]

48. Giorgio, I.; Rizzi, N.L.; Andreaus, U.; Steigmann, D.J. A two-dimensional continuum model of pantographic sheets moving in a 3D space and accounting for the offset and relative rotations of the fibers. *Math. Mech. Complex Syst.* **2019**, *7*, 311–325. [CrossRef]
49. dell'Isola, F.; Turco, E.; Misra, A.; Vangelatos, Z.; Grigoropoulos, C.; Melissinaki, V.; Farsari, M. Force–displacement relationship in micro-metric pantographs: Experiments and numerical simulations. *Comptes Rendus Mécanique* **2019**, *347*, 397–405. [CrossRef]